Pulsed-Laser Flash and Continuous Photolysis of Aqueous Solutions of Methyl Viologen, Oxalate, and Their Ion-Pair Complexes

Dasari R. Prasad,[†] Morton Z. Hoffman,*[†] Quinto G. Mulazzani,[‡] and Michael A. J. Rodgers[§]

Contribution from the Department of Chemistry, Boston University, Boston, Massachusetts 02215, Istituto di Fotochimica e Radiazioni d'Alta Energia, Consiglio Nazionale delle Ricerche, 40126 Bologna, Italy, and the Center of Fast Kinetics Research, University of Texas, Austin, Texas 78712. *Received January 21, 1986*

Abstract: MV^{2+} forms a 1:1 ion-pair complex (K_{eq} = 21 M^{-1}) with $C_2O_4^{2-}$ in aqueous solution at natural pH (7.1) that exhibits an enhanced tail absorption in the 310–400-nm region; at λ <310 nm, the apparent molar absorptivity of the complex is approximately the same as that of uncomplexed MV^{2+}. The continuous photolysis of deaerated solutions of MV^{2+} and $C_2O_4^{2-}$ at 254–380 nm generates $MV^{\bullet+}$ initially linearly with increasing irradiation time from which values of $\Phi(MV^{\bullet+})$ are obtained. $\Phi(MV^{\bullet+})$ is a function of the excitation wavelength and the fraction of light absorbed by the complex and the uncomplexed substrates; there is no evidence that light absorbed by uncomplexed MV^{2+} and $C_2O_4^{2-}$ results in any net photochemistry. Inasmuch as the oxidation of $C_2O_4^{2-}$ yields strongly reducing $CO_2^{\bullet-}$ (via the decarboxylation of ephemeral $C_2O_4^{\bullet-}$) which generates a second equivalent of $MV^{\bullet+}$, η_{cr}, the efficiency of release of redox products from the initially populated charge-transfer excited state, can be calculated; η_{cr} exhibits a long-wavelength plateau (0.12 at 340–380 nm) and rises smoothly to 0.25 at 254 nm. Pulsed-laser excitation of $C_2O_4^{2-}$ at 266 nm produces e_{aq}^- via multiphoton processes; excitation of the complex generates $MV^{\bullet+}$ within the laser pulse, followed by the formation of the second equivalent. At 355 nm, where higher concentrations of MV^{2+} are required ($\geq$1 mM), the initial transient absorption generated by the laser pulse is not that of free $MV^{\bullet+}$; its enhanced absorption in the 450–500-nm region is reminiscent of that displayed by reduced-viologen dimers and aggregates. The conversion of the initial absorption to that of free $MV^{\bullet+}$ occurs via [MV^{2+}]-independent first-order kinetics; k_{obsd} decreases with increasing [$C_2O_4^{2-}$]. Under these conditions, MV^{2+} can be visualized as existing as an aggregate surrounded by $C_2O_4^{2-}$; excitation of an ion pair eventually results in the existence of two $MV^{\bullet+}$ species within a "pseudomicelle". The final absorption change represents the formation of $MV^{\bullet+}$ in its equilibrated state in bulk solution.

Because of its role as an electron relay in systems that serve as models for the photochemical storage and conversion of solar energy,[1] methyl viologen (1,1′-dimethyl-4,4′-dipyridinium dication; MV^{2+}) continues to be the subject of investigations of its one-electron reduction to $MV^{\bullet+}$,[2-5] and of the intermediacy of the latter species in the reduction of H_2O to H_2.[6]

One aspect of the solution chemistry of MV^{2+} that appears to be important in the control of the yield of redox products in photochemical reactions[7-9] is its ability to form complexes with ionic and neutral species.[10-25] This interaction manifests as new absorption bands with discrete maxima or increased tail absorptions to the red of those of the components alone.[26] These absorptions are photochemically active; the formation of $MV^{\bullet+}$ in flash photolysis demonstrates that they are charge transfer in nature. If the donor is sacrificial, i.e. its oxidized form undergoes rapid, irreversible transformation, back-electron transfer between $MV^{\bullet+}$ and the oxidized donor, in the solvent cage or bulk solution, is minimized or eliminated, and $MV^{\bullet+}$ has long-term stability under both continuous and flash photolysis conditions.

The most widely used reductants in photochemical solar energy model systems have been EDTA and triethanolamine (TEOA); recently, the oxalate ion ($C_2O_4^{2-}$) has found use as an excited-state reductive quencher[27] and sacrificial electron donor.[28,29] As expected, $C_2O_4^{2-}$ and cationic species form ion pairs that are photochemically active;[15,30] in particular, the excitation of the $MV^{2+}/C_2O_4^{2-}$ system at 313 and 366 nm results in the formation of $MV^{\bullet+}$ with rather high quantum yields (0.2–0.3).[15] The oxidation of $C_2O_4^{2-}$ generates the ephemeral $C_2O_4^{\bullet-}$ radical, which is generally believed to undergo rapid decarboxylation[30-32] to form CO_2 and the strongly reducing $CO_2^{\bullet-}$ radical ($E°(CO_2/CO_2^{\bullet-})$ = −2.0 V);[33] $CO_2^{\bullet-}$ rapidly, quantitatively, and irreversibly reduces MV^{2+} to $MV^{\bullet+}$.[34]

As part of our continuing interest in redox processes involving components of photochemical model systems, we have undertaken a thorough investigation of the pulsed-laser flash and continuous photolysis of the $MV^{2+}/C_2O_4^{2-}$ system in aqueous solution. In

[†] Boston University
[‡] Consiglio Nazionale delle Ricerche; Visiting Scholar, Boston University.
[§] University of Texas.

(1) *Photogeneration of Hydrogen*; Harriman, A., West, M. A., Eds.; Academic Press: London, 1982; also references therein.
(2) Venturi, M.; Mulazzani, Q. G.; Hoffman, M. Z. *J. Phys. Chem.* **1984**, *88*, 912.
(3) Rodgers, M. A. J. *Radiat. Phys. Chem.* **1984**, *23*, 245.
(4) Venturi, M.; Mulazzani, Q. G.; Hoffman, M. Z. *Radiat. Phys. Chem.* **1984**, *23*, 229.
(5) Mulazzani, Q. G.; Venturi, M.; Hoffman, M. Z. *J. Phys. Chem.* **1985**, *89*, 722.
(6) *Energy Resources through Photochemistry and Catalysis*; Grätzel, M., Ed.; Academic Press: New York, 1983; also references therein.
(7) Mandal, K.; Hoffman, M. Z. *J. Phys. Chem.* **1984**, *88*, 185.
(8) Mandal, K.; Hoffman, M. Z. *J. Phys. Chem.* **1984**, *88*, 5632.
(9) Prasad, D. R.; Mandal, K.; Hoffman, M. Z. *Coord. Chem. Rev.* **1985**, *64*, 175.
(10) Hoffman, M. Z.; Prasad, D. R.; Jones, G., II; Malba, V. *J. Am. Chem. Soc.* **1983**, *105*, 6360.
(11) Prasad, D. R.; Hoffman, M. Z. *J. Phys. Chem.* **1984**, *88*, 5660.
(12) Ebbesen, T. W.; Levey, G.; Patterson, L. K. *Nature (London)* **1982**, *298*, 545.
(13) Ebbesen, T. W.; Ferraudi, G. *J. Phys. Chem.* **1983**, *87*, 3717.
(14) Ebbesen, T. W.; Manring, L. E.; Peters, K. S. *J. Am. Chem. Soc.* **1984**, *106*, 7400.
(15) Barnett, J. R.; Hopkins, A. S.; Ledwith, A. *J. Chem. Soc., Perkin Trans. 2* **1973**, *80*.
(16) Jones, G., II; Zisk, M. B. *J. Org. Chem.* **1986**, *51*, 947.
(17) Nakahara, A.; Wang, J. H. *J. Phys. Chem.* **1963**, *67*, 496.
(18) Poulos, A. T.; Kelley, C. K.; Simone, R. *J. Phys. Chem.* **1981**, *85*, 823.
(19) Poulos, A. T.; Kelley, C. K. *J. Chem. Soc., Faraday Trans. 1* **1983**, *79*, 55.
(20) White, B. G. *Trans. Faraday Soc.* **1969**, *65*, 2000.
(21) Sullivan, B. P.; Dressick, W. J.; Meyer, T. J. *J. Phys. Chem.* **1982**, *86*, 1473.
(22) Deronzier, A.; Esposito, F. *Nouv. J. Chim.* **1983**, *7*, 15.
(23) Oliveira, L. A. A.; Haim, A. *J. Am. Chem. Soc.* **1982**, *104*, 3363.
(24) Rougee, M.; Ebbesen, T.; Ghetti, F.; Bensasson, R. V. *J. Phys. Chem.* **1982**, *86*, 4404.
(25) Kuczynski, J. P.; Milosavijevic, B. H.; Lappin, A. G.; Thomas, J. K. *Chem. Phys. Lett.* **1984**, *104*, 149.
(26) *Organic Charge-Transfer Complexes*; Foster, R., Ed.; Academic Press: London, 1969.

0002-7863/86/1508-5135$01.50/0

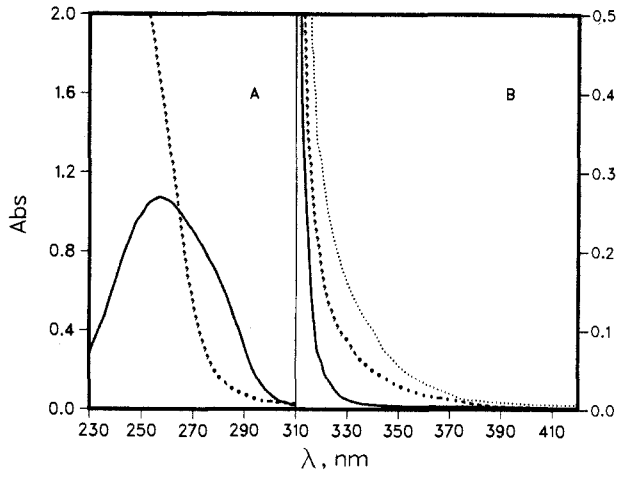

Figure 1. Absorption spectra (1-cm cell) of aqueous solutions: (A) 5.0 × 10^{-5} M MV^{2+} (—), 0.10 M $C_2O_4^{2-}$ (---); (B) 0.010 M MV^{2+} (—), 0.010 M MV^{2+} and 0.025 M $C_2O_4^{2-}$ (---), 0.010 M MV^{2+} and 0.10 M $C_2O_4^{2-}$ (···).

this work, we have measured the equilibrium constant for the formation of the 1:1 complex between MV^{2+} and $C_2O_4^{2-}$, determined the quantum yield of formation of $MV^{\bullet+}$ ($\Phi(MV^{\bullet+})$) as a function of excitation wavelength (254–380 nm) and the initial concentrations of MV^{2+} and $C_2O_4^{2-}$, and explored the fast kinetics of the processes that occur following the absorption of 266- and 355-nm light from pulsed laser sources.

Experimental Section

Materials. Methyl viologen dichloride (B.D.H.) was recrystallized several times from methanol and dried at 70 °C under vacuum for more than 24 h. $K_2C_2O_4$ (Fisher) and Na_2SO_4 (Baker Analyzed Reagent) were used without further purification. Distilled water was further purified by passage through a Millipore Purification Train.

Continuous Photolysis. Photolyses at 254 nm were performed with use of a low-pressure Hg lamp (Ultra-Violet Products, Inc.) that emits >99% of its energy at that wavelength; a 5-cm path length of acetone completely eliminated any photochemistry. For continuous photolyses at 270–310 nm, a Bausch and Lomb high-intensity monochromator in conjunction with a 1000 W Xe arc lamp was used; for 310–380 nm, a 200 W super-pressure Hg lamp served as the light source.

Solutions were contained in a 1-cm cuvette provided with a Teflon stopcock, were deoxygenated with a stream of Ar, and were stirred during photolysis by means of a small Teflon-coated magnetic bar. The intensity of light incident on the solutions was determined relative to the ferrioxalate actinometer[35] for every wavelength used; the intensity of absorbed light was determined for each sample from Beer's law. The concentration of $MV^{\bullet+}$ was determined from the absorbance of the photolyzed solutions at 605 nm, taking $\epsilon_{605} = 1.37 \times 10^4$ M^{-1} cm^{-1}.[36] Spectra were recorded on a Cary 210 spectrophotometer.

Laser Flash Photolysis. Experiments were performed at the Center for Fast Kinetics Research (CFKR), University of Texas, where Q-switched and mode-locked Nd:YAG laser were used to generate pulses of 11 and 0.2 ns, respectively, at 266 and 355 nm.[37] Spectra and kinetics were obtained from the computer averaging of 4–10 individual shots. The excitation beam passed through 1 cm of solution; the analyzing light was focussed through a pinhole approximately 1 mm from the front face of the cell. The path lengths of the analyzing light were 0.5 and 1.0 cm for 355 and 266-nm excitation, respectively. The solutions were deaerated and continuously mixed with a stream of N_2.

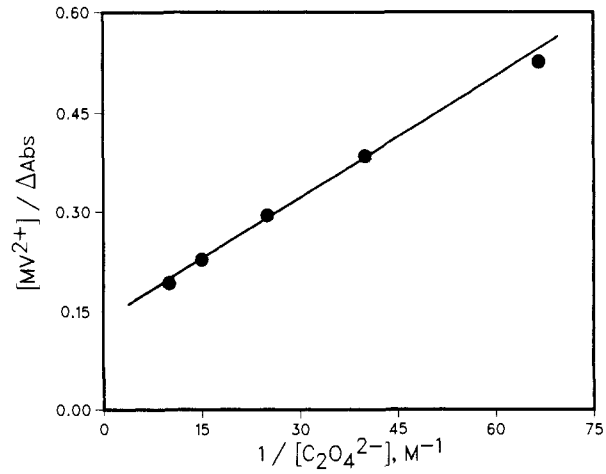

Figure 2. Benesi–Hildebrand analysis of absorption data at 350 nm for solutions containing 0.010 M MV^{2+}.

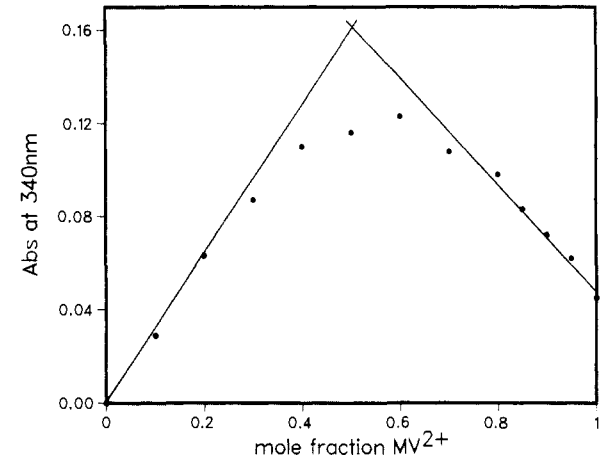

Figure 3. Job's plot for the absorbance at 340 nm for solutions at constant $[MV^{2+}] + [C_2O_4^{2-}] = 0.050$ M.

Results

Absorption Studies. As Figure 1 shows, aqueous solutions of MV^{2+} and $C_2O_4^{2-}$ exhibit enhanced absorption over that displayed by MV^{2+} alone. Below 310 nm, the spectrum of $MV^{2+}/C_2O_4^{2-}$ mixtures is dominated by that of MV^{2+}; the absorbance of solutions of $C_2O_4^{2-}$ is negligible at $\lambda > 300$ nm. Figure 1 also shows the dependence of the absorption at 310–420 nm on $[C_2O_4^{2-}]$ (0.015–0.10 M) at fixed $[MV^{2+}]$ (0.010 M); the spectra are unchanged in the pH range 7.1–10.0. Use of the Benesi–Hildebrand analysis[38] for 1:1 donor–acceptor complexes (Figure 2) for the absorbance at 350 nm yields $K_{eq} = 21$ M^{-1} and $\epsilon_{350} = 7.2$ M^{-1} cm^{-1} at the ambient pH of these solutions (7.1); the linearity of the plot demonstrates that K_{eq} is constant within the range of the ionic strengths (0.08–0.33 M) of the solutions. Further evidence that the absorbing complex has a 1:1 stoichiometry comes from Job's plots of the absorbance of the system at 340 nm as a function of the mole fraction of MV^{2+} at constant ($[MV^{2+}] + [C_2O_4^{2-}]$) = 0.050 M (Figure 3). Knowledge of the values of K_{eq} and ϵ_λ enables the equilibrium concentrations of all three components, and their contributions to the total absorbance at each wavelength, to be calculated. For example, the absorption of the solutions at 254 nm fits Beer's law when measured ϵ-values of $C_2O_4^{2-}$ (25 M^{-1} cm^{-1}) and MV^{2+} (1.84×10^4 M^{-1} cm^{-1}) are coupled with a calculated value for the complex of 2×10^4 M^{-1} cm^{-1}.

(27) Bliese, M.; Launikonis, A.; Loder, J. W.; Mau, A. W.-H.; Sasse, W. H. F. *Aust. J. Chem.* **1983**, *36*, 1873.
(28) Furlong, D. N.; Wells, D.; Sasse, W. H. F. *J. Phys. Chem.* **1985**, *89*, 1922.
(29) Rubinstein, I.; Bard, A. J. *J. Am. Chem. Soc.* **1981**, *103*, 512.
(30) Pina, F.; Mulazzani, Q. G.; Venturi, M.; Ciano, M.; Balzani, V. *Inorg. Chem.* **1985**, *24*, 848.
(31) Farhataziz; Ross, A. B. *Natl. Stand. Ref. Data Ser. (U.S. Natl. Bur. Stand.)* **1977**, *No. 59*.
(32) Chang, M.-M.; Saji, T.; Bard, A. J. *J. Am. Chem. Soc.* **1977**, *99*, 5399.
(33) Breitenkamp, M.; Henglein, A.; Lilie, J. *Ber. Bunsenges. Phys. Chem.* **1976**, *80*, 973.
(34) Farrington, J. A.; Ebert, M.; Land, E. J.; Fletcher, K. *Biochim. Biophys. Acta* **1973**, *314*, 372.
(35) Calvert, J. G.; Pitts, J. N., Jr. *Photochemistry*; Wiley: New York, 1966; p 784.
(36) Watanabe, T.; Honda, K. *J. Phys. Chem.* **1982**, *86*, 2617.
(37) Foyt, D. C. *Comput. Chem.* **1981**, *5*, 49.
(38) Benesi, H. A.; Hildebrand, J. H. *J. Am. Chem. Soc.* **1949**, *71*, 2703.

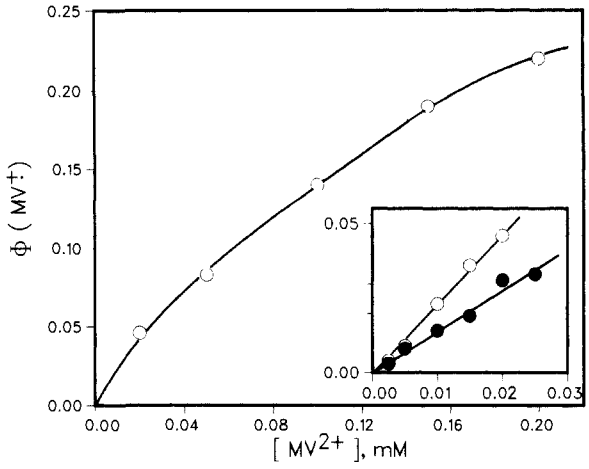

Figure 4. $\Phi(MV^{\bullet+})$ as a function of $[MV^{2+}]$ upon the 254-nm photolysis of deaerated solutions containing 0.10 (○) and 0.20 M (●) $C_2O_4^{2-}$.

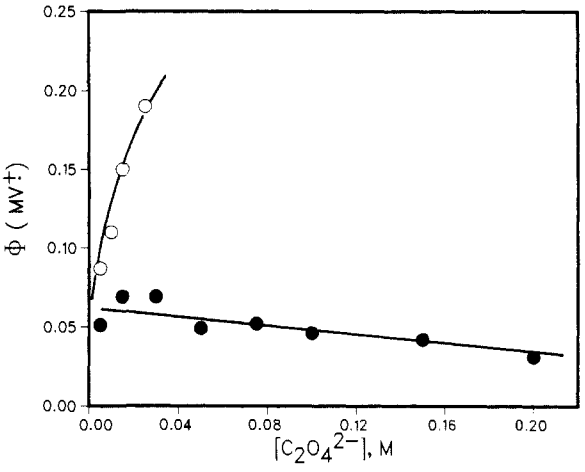

Figure 5. $\Phi(MV^{\bullet+})$ as a function of $[C_2O_4^{2-}]$ upon the 254-nm photolysis of deaerated solutions containing 0.020 (○) and 0.20 mM (●) MV^{2+}.

Quantum Yield Measurements. The continuous photolysis of deaerated solutions of MV^{2+} in the absence of $C_2O_4^{2-}$ at 254 nm does not yield any $MV^{\bullet+}$. The photolysis of deaerated solutions of MV^{2+} and $C_2O_4^{2-}$ at 254–380 nm leads to the formation of $MV^{\bullet+}$, initially linearly with irradiation time; in the absence of air, $MV^{\bullet+}$ is stable. Values of $\Phi(MV^{\bullet+})$ were determined from the ratio of the initial rate of $MV^{\bullet+}$ formation to the rate of light absorption and were reproducible to within ±10–15%.

The values of $\Phi(MV^{\bullet+})$ as a function of excitation wavelength (254–380 nm) and the initial concentrations of MV^{2+} and $C_2O_4^{2-}$ are presented in Table I. For 254-nm irradiation, it is clear that $\Phi(MV^{\bullet+})$ is a complex function of the concentrations. Figure 4 shows the dependence of $\Phi(MV^{\bullet+})$ on $[MV^{2+}]$ at constant $[C_2O_4^{2-}]$ (0.10 and 0.20 M); an experiment with 0.020 mM MV^{2+}, 0.10 M $C_2O_4^{2-}$, and 0.10 M Na_2SO_4 caused no change in the observed value of Φ. Figure 5 shows the effects of the variation of $[C_2O_4^{2-}]$ (0.0050–0.20 M) at constant $[MV^{2+}]$ (0.020 and 0.20 mM) on $\Phi(MV^{\bullet+})$. On the other hand, the data at 340 nm for solutions containing 5.0–25 mM MV^{2+} and 0.10 M $C_2O_4^{2-}$ show no systematic variation in $\Phi(MV^{\bullet+})$, with an average value of 0.23 and an average deviation of ±13%. It should be noted that our measured values of $\Phi(MV^{\bullet+})$ at 310 and 360 nm are virtually the same as those previously reported[15] at 313 and 366 nm under very similar concentration conditions.

Flash Experiments. 266-nm Excitation. The flash photolysis of a 0.10 mM MV^{2+} solution ($\epsilon_{266} = 1.67 \times 10^4$ M^{-1} cm^{-1}) yielded no detectable transient absorption between 350 and 600 nm in 0.1 μs.

The excitation of 0.10 M $C_2O_4^{2-}$ ($\epsilon_{266} = 10$ M^{-1} cm^{-1}) resulted, within 70 ns, in the formation of a broad absorption extending to ~450 nm from a maximum at ~720 nm; the spectrum is characteristic of the hydrated electron, e_{aq}^-.[39] The absorption, monitored at 650 nm, increases with increasing $[C_2O_4^{2-}]$ and approaches a plateau at 0.25 M. The transient absorption decays via clean first-order kinetics with k_{obsd} proportional to $[C_2O_4^{2-}]$; at high laser intensities, a second-order component is seen in the initial portion of the decay. A plot of k_{obsd} vs. $[C_2O_4^{2-}]$ (0.00–0.25 M) yields a straight line with a zero intercept and a slope = 4.6×10^7 M^{-1} s^{-1}, independent of laser flash intensity. In the presence of air, the rate of decay of e_{aq}^- is faster.

The excitation of a solution containing 0.10 mM MV^{2+} and 0.010 M $C_2O_4^{2-}$ resulted in the formation of an absorption with maxima in the 395- and 600-nm regions in less than 3 ns; a secondary first-order formation of the absorption occurred in the 10–20 μs time frame. A careful comparison of the absorption measured 0.4 and 12 μs after the 11-ns flash revealed that the 600-nm band of the initial spectrum was slightly blue-shifted relative to that of the final spectrum; furthermore, the 400–500-nm region did not grow with time although the peaks at 395 and 600 nm did. In fact, it would appear that at 420–430 nm, the final spectrum is less intense than the initial one, with isosbestic points evident.

The rate constants of the secondary growth of the absorption were determined at 395 and/or 600 nm as a function of $[MV^{2+}]$, $[C_2O_4^{2-}]$, and pH. For solutions containing 0.10 mM MV^{2+} and

Table I. $\Phi(MV^{\bullet+})$ as a Function of Excitation Wavelength and the Initial Substrate Concentrations

λ, nm	$[MV^{2+}]$, mM	$[C_2O_4^{2-}]$, M	f_1	f_2	f_3	$\Phi(MV^{\bullet+})$[a,b]
380	20	0.10	>0.99	<0.01	0.00	0.22 (1)
360	20	0.10	>0.99	>0.01	0.00	0.23 (1)
340	5.0	0.10	>0.99	<0.01	0.00	0.22 (2)
	10	0.10	>0.99	<0.01	0.00	0.17 (2)
	15	0.10	>0.99	<0.01	0.00	0.28 (2)
	20	0.10	>0.99	<0.01	0.00	0.24 (3)
	25	0.10	>0.99	<0.01	0.00	0.29 (1)
320	20	0.10	0.87	0.13	0.00	0.27 (2)
310	20	0.10	0.76	0.24	0.00	0.29 (1)
	5.0	0.10	0.75	0.24	0.01	0.23 (2)
290	0.32	0.10	0.67	0.30	0.03	0.21 (2)
270	0.085	0.10	0.54	0.22	0.24	0.20 (5)
254	0.020	0.0050	0.077	0.67	0.25	0.051 (1)
	0.020	0.015	0.13	0.37	0.50	0.069 (1)
	0.020	0.030	0.14	0.20	0.67	0.069 (1)
	0.020	0.050	0.12	0.11	0.76	0.049 (1)
	0.020	0.075	0.11	0.065	0.83	0.052 (1)
	0.020	0.10	0.097	0.038	0.87	0.046 (4)
	0.020	0.15	0.072	0.022	0.91	0.042 (1)
	0.020	0.20	0.059	0.014	0.93	0.031 (2)
	0.20	0.0050	0.10	0.87	0.033	0.087 (1)
	0.20	0.010	0.17	0.77	0.062	0.11 (1)
	0.20	0.015	0.23	0.67	0.092	0.15 (1)
	0.20	0.025	0.31	0.55	0.14	0.19 (1)
	0.0025	0.10	0.013	0.006	0.98	0.004 (1)
	0.050	0.10	0.026	0.011	0.96	0.009 (1)
	0.010	0.10	0.050	0.022	0.93	0.023 (2)
	0.015	0.10	0.072	0.033	0.90	0.036 (1)
	0.050	0.10	0.20	0.084	0.72	0.083 (1)
	0.10	0.10	0.31	0.13	0.56	0.14 (1)
	0.15	0.10	0.37	0.17	0.46	0.19 (1)
	0.20	0.10	0.44	0.17	0.39	0.22 (1)
	0.0025	0.20	0.008	0.002	0.99	0.003 (1)
	0.0050	0.20	0.016	0.004	0.98	0.008 (1)
	0.010	0.20	0.031	0.007	0.96	0.014 (2)
	0.015	0.20	0.045	0.010	0.94	0.019 (1)
	0.025	0.20	0.073	0.017	0.91	0.033 (1)

[a] Numbers in parentheses represent the number of individual runs. [b] Averages of more than one run.

(39) Matheson, M. S.; Dorfman, L. M. *Pulse Radiolysis*; The M.I.T. Press: Cambridge, MA, 1969; p 68.

Table II. Rate Constants of the Secondary Spectral Changes in the 266-nm Laser Flash Photolysis of N_2-Purged $MV^{2+}/C_2O_4^{2-}$ Aqueous Solutions as a Function of the Initial Substrate Concentrations and Beam Intensity[a]

$[MV^{2+}]$, mM	$[C_2O_4^{2-}]$, M	% beam	$k_{obsd} \times 10^{-5}$, s^{-1}
0.010	0.010	22	1.7
0.025	0.010	22	1.9
0.030	0.010	22	2.3
0.050	0.010	22	2.6
0.10	0.010	22	3.5
0.10	0.010	100	3.5
0.15	0.010	22	3.8
0.20	0.010	22	4.3
0.10	0.050	22	3.6[b]
0.10	0.0050–0.40	22	3.4[c]
0.010	0.10	6.4	1.1
0.010	0.10	22	1.9
0.010	0.10	100	4.0
0.030	0.10	22	1.5
0.050	0.10	22	2.0
0.10	0.10	22	3.2
0.15	0.10	22	4.3
0.20	0.10	22	5.3

[a] Natural pH and pH 9; averages of 1–10 individual experiments. [b] pH 3–11. [c] pH 8.0 ± 0.2 in 2×10^{-3} M HPO_4^{2-}.

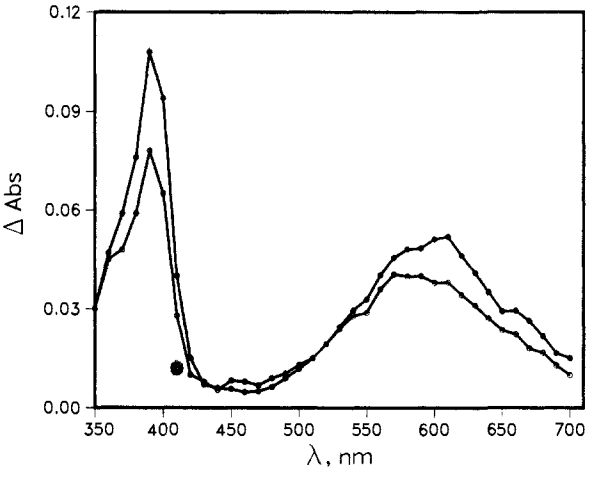

Figure 6. Absorption resulting from the 355-nm laser flash photolysis of deaerated solutions containing 15 mM MV^{2+} and 0.10 M $C_2O_4^{2-}$. Time after the flash: 0.10 μs (○); 13.5 μs (●).

0.050 M $C_2O_4^{2-}$, $k_{obsd} = (3.6 \pm 0.4) \times 10^5$ s^{-1} at pH 3–11; the presence of 0.010 M $C_2O_4^{2-}$ caused no change in the value. At pH 8.0 ± 0.2 in the presence of 2×10^{-3} M HPO_4^{2-} and 0.10 mM MV^{2+}, $k_{obsd} = (3.4 \pm 0.2) \times 10^5$ s^{-1} for $[C_2O_4^{2-}] = 0.005$–0.4 M. Table II presents the values of k_{obsd} as a function of $[MV^{2+}]$ for solutions containing 0.010, 0.050, and 0.10 M $C_2O_4^{2-}$ at ambient pH. When the solution is oxalate-rich (0.010 mM MV^{2+} and 0.10 M $C_2O_4^{2-}$), the initial absorption of e_{aq}^- is observed which decays rapidly in less than 1 μs. At 0.030 mM MV^{2+} and 0.10 M $C_2O_4^{2-}$, the absorption of e_{aq}^- is barely visible, and it decays too rapidly for its kinetics to be monitored.

Flash Experiments. 355-nm Excitation. The absorbances (1-cm path length) of the solutions at 355 nm ranged between 0.1 and 0.4, depending on the concentrations of MV^{2+} and $C_2O_4^{2-}$.

The flash photolysis of solutions containing MV^{2+} and $C_2O_4^{2-}$ at ambient pH resulted in the instantaneous formation of an absorbing species with maxima in the 395- and 600-nm regions; Figure 6 shows the absorption spectrum measured 0.10 μs after the pulse for a N_2-purged solution containing 15 mM MV^{2+} and 0.10 M $C_2O_4^{2-}$. Over the course of the next 10 μs, the absorbance of the maxima increased according to well-defined first-order kinetics; a concomitant decrease in absorbance was observed in the 450–500-nm region with isosbestic points at 440 and 520 nm. The final spectrum in Figure 6 was stable in the absence of air.

The fraction of the final absorption that originates in the slow secondary step is ~0.4 at 395 nm and ~0.3 at 605 nm, independent of $[MV^{2+}]$ (1.0–25 mM), $[C_2O_4^{2-}]$ (0.10–1.0 M), and the intensity of the excitation pulse (6.4–100% of the beam). Table III displays the observed rate constant of the secondary step which is independent ($k_{obsd} = (7.8 \pm 0.8) \times 10^5$ s^{-1}) of the monitoring wavelength, the intensity of the excitation pulse, and $[MV^{2+}]$ at constant $[C_2O_4^{2-}]$ (0.10 M); the rate constant decreases with increasing $[C_2O_4^{2-}]$ at constant $[MV^{2+}]$ (25 mM) as seen in Figure 7.

Table III. Rate Constants of the Secondary Spectral Changes in the 355-nm Laser Flash Photolysis of N_2-Purged $MV^{2+}/C_2O_4^{2-}$ Aqueous Solutions as a Function of the Initial Substrate Concentrations, Monitoring Wavelength, and Beam Intensity[a]

$[MV^{2+}]$, mM	$[C_2O_4^{2-}]$, M	λ_{mon}, nm	% beam	$k_{obsd} \times 10^{-5}$, s^{-1}	k_{av}, s^{-1}
1.0	0.10	395	29	8.8	
		395	100	8.0	
		605	100	7.8	8.2×10^5
5.0	0.10	395	29	6.3	
		605	29	6.9	
		395	100	7.2	
		605	100	6.1	6.6×10^5
15	0.10	605	29	8.4	
		610	29	7.9	
		500	29	6.6	
		395	29	9.4	8.1×10^5
25	0.10	395	29	7.8	
		605	29	8.7	8.3×10^5
25	0.74	395	29	5.5[b]	
		395	29	5.2[c]	
		395	29	5.4	
		605	29	5.4	5.4×10^5
25	1.0	395	6.4	3.9	
		395	29	4.0	
		395	100	4.4	
		605	29	5.0	
		605	29	4.3	
		605	100	4.6	4.4×10^5

[a] Average of 4–10 shots. [b] Air-saturated solution; decay of $MV^{\cdot+}$ resolved at longer times. [c] Partially deaerated.

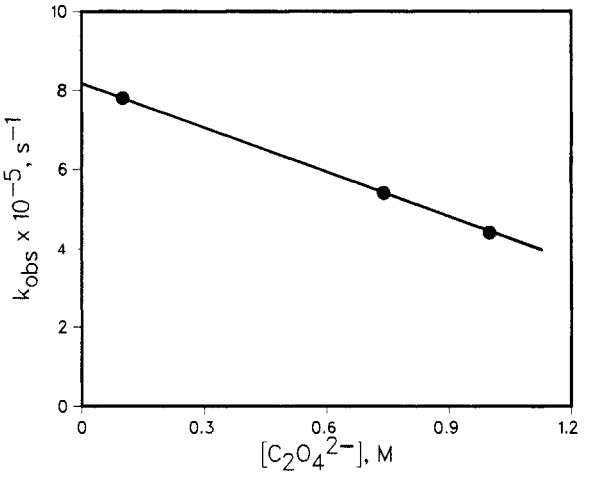

Figure 7. Dependence of the observed first-order rate constant on $[C_2O_4^{2-}]$ at constant $[MV^{2+}]$ (25 mM) for the formation of the secondary absorption upon 355-nm laser flash photolysis.

Discussion

It has been amply demonstrated that aqueous solutions of MV^{2+} and anions contain ion-pair complexes in equilibrium with the free, unbound species. The absorption of light by such a system involves the excitation of some or all of those species depending, of course, on their relative absorbances at the wavelength of irradiation; the concentrations of the absorbing species are governed by the value of the equilibrium constant and the initial concentrations of the complexing species. At each wavelength, the fractions of light

absorbed by the complex, uncomplexed MV^{2+}, and uncomplexed anion are f_1, f_2, and f_3, respectively; $f_i = A_i/A_t$, where A_i and A_t are the absorbances of the ith component and the total solution, respectively, with $A_t = \sum A_i$. Values of f_1, f_2, and f_3 are included in Table I.

Complexation Equilibrium. The tail absorption in the near-UV that is observed in the $MV^{2+}/C_2O_4^{2-}$ system, which is virtually identical in intensity with those seen for MV^{2+}/EDTA and other carfboxylates,[10,11,15,16,25] results from a 1:1 complex formed between the component species; higher aggregates, if they were to exist, apparently do not contribute to the optical absorption. The value of ϵ for the $MV^{2+}/C_2O_4^{2-}$ complex in the 250-nm region is virtually the same as that for MV^{2+} alone,[36] indicating that absorption by the complex at those wavelengths is into predominantly MV^{2+}-localized states.

The value of the equilibrium constant for the formation of the $MV^{2+}/C_2O_4^{2-}$ absorbing complex (reaction 1; $K_1 = 21\ M^{-1}$) is considerably larger than those for other MV^{2+}/dicarboxylate complexes,[16] perhaps due to the relative compactness of $C_2O_4^{2-}$, thereby enhancing the electrostatic interaction.

$$MV^{2+} + C_2O_4^{2-} \rightleftarrows [MV^{2+},C_2O_4^{2-}] \qquad (1)$$

Excitation of MV^{2+}. MV^{2+} does not exhibit any fluorescence; there appears to be no question that the emission at 525 nm observed[19,25] in solutions of MV^{2+} arises from pyridone impurities originally in the samples, or from those generated thermally or photochemically during the manipulation of the material.[11,40] The analogous compound, diquat (6,7-dihydrodipyrido[1,2-*a*:2′,1′-*c*]pyrazine dication), does exhibit a genuine fluorescence with an estimated excited-state lifetime of 1–2 ns;[40] the lack of fluorescence from MV^{2+} implies that its excited state is several orders of magnitude shorter lived, and may be in the ps or sub-ps regime. As a result, the quenching of $^*MV^{2+}$ via bimolecular reaction with, say, $C_2O_4^{2-}$ would be highly improbable for the concentrations of $C_2O_4^{2-}$ used in this study, even if the quenching rate constant were as large as that for diquat ($2.9 \times 10^{10}\ M^{-1}\ s^{-1}$).[41] Thus, any light absorbed directly by MV^{2+} can be regarded as chemically nonproductive.

Excitation of $C_2O_4^{2-}$. The UV photolysis of simple inorganic anions in aqueous solution can give rise to the formation of e_{aq}^- if the absorption of light results in charge-transfer-to-solvent excitation;[42] in the case of I^-, the yield of e_{aq}^- at 254 nm is quite high (0.3).[43] For $C_2O_4^{2-}$, photoionization does not appear to be an important process under steady-state illumination. In fact, we will regard any light absorbed directly by $C_2O_4^{2-}$ as nonproductive; the rather high yield of e_{aq}^- obtained upon the 266-nm laser flash photolysis of $C_2O_4^{2-}$ can be attributed to multiphotonic excitation. The disappearance of e_{aq}^- reflects its well-known second-order decay at high $[e_{aq}^-]$ and its scavenging by $C_2O_4^{2-}$ and O_2.[44]

Excitation of $MV^{2+}/C_2O_4^{2-}$. In its simplest terms, the absorption of the fraction of incident light f_1 by the $[MV^{2+},C_2O_4^{2-}]$ ion-pair complex (reaction 2) results in the generation of a charge-transfer excited state that can be viewed as a geminate radical pair contained in a solvent cage, $[MV^{\bullet+},C_2O_4^{\bullet-}]$. Unless release of the radical pair into the bulk solution (reaction 3) occurs competitively with back-electron transfer within the solvent cage (reaction 4), solvent-separated redox products will not form. The irreversible transformation of $C_2O_4^{\bullet-}$ (reaction 5) into CO_2 and $CO_2^{\bullet-}$, species that cannot engage in back-electron transfer with $MV^{\bullet+}$, permits the radical cation to accumulate. In reaction 6, $CO_2^{\bullet-}$ reduces $MV^{\bullet+}$, undoubtedly both complexed and uncomplexed, to generate a second equivalent of $MV^{\bullet+}$; k_6 is known from pulse radiolysis to be in the range $0.4–1.6 \times 10^{10}\ M^{-1}\ s^{-1}$, depending upon the ionic strength and composition of the solution.[34,45]

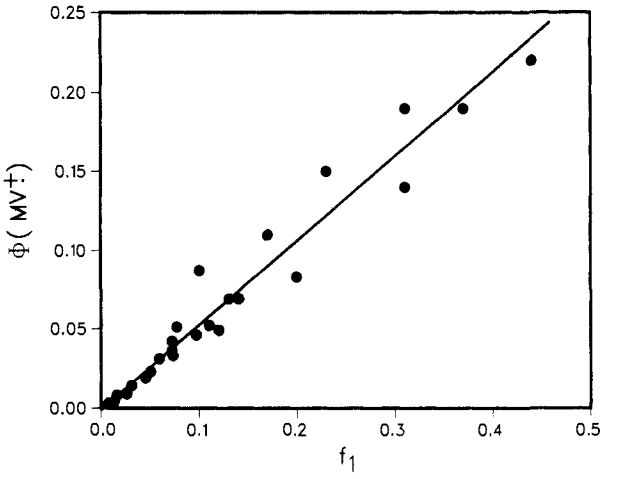

Figure 8. $\Phi(MV^{\bullet+})$ as a function of f_1 for irradiation at 254 nm.

Reaction 7 describes the back-electron transfer between the redox pair that serves to destroy the accumulated $MV^{\bullet+}$. From reactions 2–7, $\Phi(MV^{\bullet+}) = 2f_1\eta_{cr}(1 - \eta_b)$, where η_{cr} is the efficiency of release of the redox products from the solvent cage, $k_3/(k_3 + k_4)$, and η_b is the efficiency of bulk solution back electron transfer, $k_7[MV^{\bullet+}]/(k_5 + k_7[MV^{\bullet+}])$.

$$[MV^{2+},C_2O_4^{2-}] \xrightarrow{h\nu} [MV^{\bullet+},C_2O_4^{\bullet-}] \qquad (2)$$

$$[MV^{\bullet+},C_2O_4^{\bullet-}] \rightarrow MV^{\bullet+} + C_2O_4^{\bullet-} \qquad (3)$$

$$[MV^{\bullet+},C_2O_4^{\bullet-}] \rightarrow [MV^{2+},C_2O_4^{2-}] \qquad (4)$$

$$C_2O_4^{\bullet-} \rightarrow CO_2^{\bullet-} + CO_2 \qquad (5)$$

$$MV^{2+} + CO_2^{\bullet-} \rightarrow MV^{\bullet+} + CO_2 \qquad (6)$$

$$MV^{\bullet+} + C_2O_4^{\bullet-} \rightarrow MV^{2+} + C_2O_4^{2-} \qquad (7)$$

Values of k_5 and k_7 have not been previously reported. In an independent attempt to evaluate these rate constants, we have examined the pulse and continuous radiolysis of aqueous solutions containing $C_2O_4^{2-}$ and MV^{2+}.[45] The product of the interaction of ·OH radicals with $C_2O_4^{2-}$, which is presumed to be $C_2O_4^{\bullet-}$,[46] generates $CO_2^{\bullet-}$ with $k \sim 2 \times 10^6\ s^{-1}$; this species reacts with $MV^{\bullet+}$ with $k \sim 7 \times 10^{10}\ M^{-1}\ s^{-1}$. While it is tempting to assign these values to k_5 and k_7, respectively, the oxidative addition of ·OH to $C_2O_4^{2-}$ must be regarded as a distinct possibility. In fact, if these values of k_5 and k_7 are used to evaluate η_b, it is predicted that no more than 3 μM $MV^{\bullet+}$ could accumulate before $\Phi(MV^{\bullet+})$ fell off by more than 10% of its initial value; at 10 μM $MV^{\bullet+}$, the fall off would be predicted to occur to an extent greater than 25%. These predictions are not supported by the continuous photolysis results in which linear $MV^{\bullet+}$ production and, hence, constant $\Phi(MV^{\bullet+})$ are observed even up to 30 μM $MV^{\bullet+}$. One must conclude that the species formed from the reaction of ·OH with $C_2O_4^{2-}$ is not $C_2O_4^{\bullet-}$, and that the value of k_5 is $>10^8\ s^{-1}$. The linear generation of $MV^{\bullet+}$ during the initial phases of the continuous photolysis, from which the values of $\Phi(MV^{\bullet+})$ are calculated, argues that back-electron-transfer reaction 7 can be ignored when $[MV^{\bullet+}]$ is low.

In the 340–380-nm region, the only absorbing species is the $MV^{2+}/C_2O_4^{2-}$ complex; the fraction of light absorbed by uncomplexed MV^{2+} and $C_2O_4^{2-}$ is <0.01. The values of $\Phi(MV^{\bullet+})$ thus obtained (Table I) yield an average value of 0.24, with an average deviation of ±11%, independent of the concentration of the complex (3.2–13 mM) and uncomplexed MV^{2+} (1.8–12 mM) at essentially constant $[C_2O_4^{2-}]$ (0.10 M). For excitation at <320 nm, uncomplexed MV^{2+} begins to absorb competitively; at <290

(40) Novakovic, V.; Hoffman, M. Z., manuscript in preparation.
(41) Hopkins, A. S.; Ledwith, A.; Stam, M. F. *Chem. Commun.* **1970**, 494.
(42) Fox, M. In *Concepts of Inorganic Photochemistry*; Adamson, A. W., Fleischauer, P. D., Eds.; Wiley: New York, 1975; p 333.
(43) Jortner, J.; Ottolenghi, M.; Stein, G. *J. Phys. Chem.* **1962**, *66*, 2029.
(44) Anbar, M.; Bambenek, M.; Ross, A. B. *Natl. Stand. Ref. Data Ser. (U.S. Natl. Bur. Stand.)* **1973**, *No. 43*.
(45) Mulazzani, Q. G.; D'Angelantonio, M.; Venturi, M.; Hoffman, M. Z.; Rodgers, M. A. J. *J. Phys. Chem.*, in press.
(46) Draganic, I. G.; Gal, O. *Radiat. Res. Rev.* **1971**, *3*, 167 and references therein.

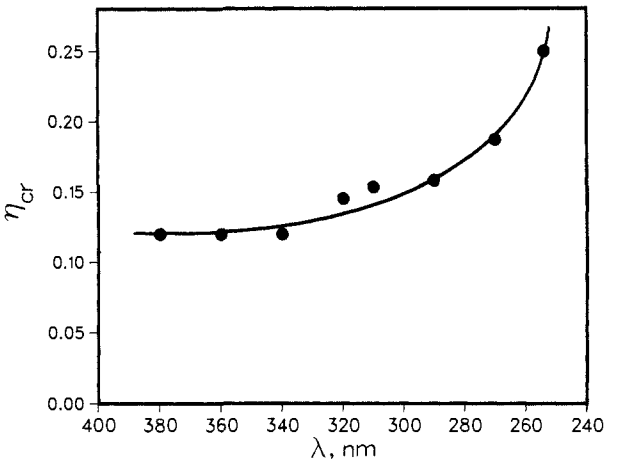

Figure 9. Plot of average values of η_{cr} as a function of excitation wavelength.

nm, the absorption of uncomplexed $C_2O_4^{2-}$ becomes significant; at 254 nm, all three components of the solution absorb competitively. As a result, at 254 nm, the dependences of $\Phi(MV^{\bullet+})$ on the substrate concentrations shown in Figures 4 and 5 are very complex. In order to obtain values of the quantum yield for the excitation of the $MV^{2+}/C_2O_4^{2-}$ complex, it is necessary to correct the observed quantum yields for the inner filter effect; $\Phi_{cor} = \Phi_{obs}/f_1$. In doing so, it is assumed that absorption of light by uncomplexed MV^{2+} and $C_2O_4^{2-}$ does not lead to net photochemistry; this assumption is supported by the linear relationship between $\Phi(MV^{\bullet+})$ and f_1 (Figure 8) where the line extrapolates to a value of $\Phi(MV^{\bullet+}) \sim 0.5$ at $f_1 = 1$. If the absorption of continuous radiation by $C_2O_4^{2-}$ were to generate e_{aq}^- via reaction 8 with an efficiency of η_8, competitive scavenging of e_{aq}^- by MV^{2+} and $C_2O_4^{2-}$ (reactions 9 and 10; k_9 and k_{10} are reported to be 8.4×10^{10} and $1.7\text{–}4.8 \times 10^7$ M^{-1} s^{-1}, respectively)[34,44] would lead to additional sources of $MV^{\bullet+}$. We know[45] that the reaction of the reduction products of reaction 10 ($P^{\bullet-}$) with MV^{2+} rapidly produces $MV^{\bullet+}$ (reaction 11). Thus, if reactions 6 and 8–11 were important sources of $MV^{\bullet+}$ when f_3 were large, $\Phi(MV^{\bullet+})$ would approach a limiting value of $2f_3\eta_8$. From the data in Figure 4, we see that the limiting value of $\Phi(MV^{\bullet+})$ and, thus, η_8 is, or is close to, zero.

$$C_2O_4^{2-} \xrightarrow{h\nu} e_{aq}^- + CO_2^{\bullet-} + CO_2 \quad (8)$$

$$e_{aq}^- + MV^{2+} \rightarrow MV^{\bullet+} \quad (9)$$

$$e_{aq}^- + C_2O_4^{2-} \rightarrow P^{\bullet-} \quad (10)$$

$$MV^{2+} + P^{\bullet-} \rightarrow MV^{\bullet+} + P \quad (11)$$

Wavelength Dependence of η_{cr}. The measured values of $\Phi(MV^{\bullet+})$, when corrected for the fractional absorption by the complex, are a function of λ_{exc}; values of η_{cr} are obtained from $\Phi(MV^{\bullet+})$ and f_1 under conditions where η_b is negligibly small (Figure 9). At 254 nm, an average value of η_{cr} of 0.25 with an average deviation of ±13% is calculated for 24 separate experiments (after eliminating the single point that lies outside 2σ from the mean); at 340–380 nm, η_{cr} exhibits a plateau value of 0.12. Compared to other ion-pair complexes of similar charge,[16] the values of η_{cr} exhibited for the $MV^{2+}/C_2O_4^{2-}$ system are quite high. From the point of view of the mechanism presented in reactions 2–6, this results means that the values of k_3 and k_4 are of the same order of magnitude; cage release of the redox pair (reaction 3) is generally regarded as occurring in the sub-ns time frame.[47] Although k_3 is undoubtedly a function of solution medium, the charges on the redox pair, and their distance of separation, the differences in the values of η_{cr} for oxalate and other dicarboxylates[16] could arise from two factors: variation in k_4 due to differences in the electronic factors associated with electron trnasfer[48] and differences in the extent to which irreversible decomposition of one of the radical-pair partners occurs within the solvent cage. This latter factor, at least to some extent, is an attractive possibility for $C_2O_4^{\bullet-}$ (reaction 12).

$$[MV^{\bullet+}, C_2O_4^{\bullet-}] \rightarrow MV^{\bullet-} + CO_2^{\bullet-} + CO_2 \quad (12)$$

It is well established that η_{cr} for CT complexes increases with increasing photon energy,[49–52] although the particular functionality involving a long-wavelength plateau disclosed here does not appear to have been reported before; we have found that the photolysis of the MV^{2+}/EDTA system shows the same effect.[53] An examination of Figures 1 and 9 reveals that the long-wavelength plateau occurs in the spectral region corresponding to the new absorption by the ion-pair complex, while the sharp rise in the value of η_{cr} takes place in the MV^{2+}-localized absorption of the complex. It can be argued that selective excitation generates species with different geometries and, hence, reactivities toward cage separation and electron transfer.

Two other more complex models to account for this wavelength effect have been discussed:[52] (1) at long wavelengths, the system remains in the initially populated excited singlet CT state inasmuch as it is not sufficiently vibrationally excited to cross to the excited triplet CT state; this model reasonably assumes that the ^{1}CT state is shorter lived than is the ^{3}CT state with regard to their decays to the ground state via geminate cage back-electron transfer (reaction 3). As shorter excitation wavelengths are employed, intersystem crossing becomes more probable; the model predicts the appearance of a high-photon energy plateau representing total population of ^{3}CT which, however, our data does not display. (2) Absorption of photon energy populates a series of vibronic levels which are dissociative with respect to ion-pair separation; the different levels couple in different ways with vibrational modes of the molecules and phonon modes of the solvent. In a manner similar to the first model, a low-photon-energy plateau is possible depending on the lifetimes of the levels relative to relaxation and cage separation.

Fast Kinetics. Hydrated electrons, generated in reaction 8 by the 266-nm multiphoton excitation of $C_2O_4^{2-}$ in the absence of MV^{2+}, decay via reaction 10 with a rate constant of 4.6×10^7 M^{-1} s^{-1}, a value that is within the range of those previously reported.[44] In the presence of MV^{2+}, the yield of e_{aq}^- is decreased due to the decrease in the value of f_3, and its rate of decay is increased due to the competition of reaction 9.

The excitation of the $MV^{2+}/C_2O_4^{2-}$ ion-pair complex at 266 nm generates an initial absorption that appears within the time of the laser flash; it represents the $MV^{\bullet+}$ species that is released into solution by reaction 3. When $[MV^{2+}] = 10$ μM, the first-order rate constant for the formation of the final $MV^{\bullet+}$ species, monitored at 600 nm, depends on the intensity of the laser beam (Table II), doubtlessly indicating the complexities that exist for multiphoton excitation in an optically opaque solution. As $[MV^{2+}]$ is increased, k_{obsd} increases. At 50–100 μM MV^{2+}, $k_{obsd}/[MV^{2+}] \sim 3\text{–}4 \times 10^9$ M^{-1} s^{-1}, a value that approximates k_6 determined pulse radiolytically for solutions containing 0.5–1.0 M $C_2O_4^{2-}$ and 0.2 M HCO_2^-;[45] $k_{obsd}/[MV^{2+}]$ is independent of pH (3–11) and $[C_2O_4^{2-}]$ as expected for reaction 6. However, at $[MV^{2+}] > 100$ μM, $k_{obsd}/[MV^{2+}]$ is significantly less than that value, becoming almost a factor of 2 less at 200 μM MV^{2+}. It appears that, although the secondary formation of the $MV^{\bullet+}$ species can be generally identified with reaction 6, the system becomes unexpectedly complex as $[MV^{2+}]$ is increased.

This conclusion becomes secure when the results of the 355-nm laser experiments are examined. At the higher concentrations

(47) Balzani, V.; Scandola, F. In *Energy Resources through Photochemistry and Catalysis*; Grätzel, M., Ed.; Academic press: New York, 1983; p 1.

(48) Newton, M. D.; Sutin, N. *Annu. Rev. Phys. Chem.* **1984**, *35*, 437.
(49) Jones, G., II; Becker, W. G. *J. Am. Chem. Soc.* **1981**, *103*, 4630.
(50) Jones, G., II; Becker, W. G. *Chem. Phys. Lett.* **1982**, *85*, 271.
(51) Jones, G., II; Becker, W. G. *J. Am. Chem. Soc.* **1983**, *105*, 1276.
(52) Jones, G., II; Malba, V. *Chem. Phys. Lett.* **1985**, *119*, 105.
(53) Prasad, D. R.; Hoffman, M. Z. *J. Chem. Soc., Faraday Trans.*, in press.

of MV^{2+} employed, necessitated by the absorbance requirements, the formation of the second equivalent of $MV^{\bullet+}$ via reaction 6 should occur in the ns time frame. Even with the use of the mode-locked laser, no secondary formation of the 600-nm absorption was observed at short times after the pulse. As shown in Table III, a secondary formation *is* observed, but in the μs time frame. This secondary formation, which *cannot* be attributed to reaction 6, is observed at 395 and 605 nm, and is independent of beam intensity and $[MV^{2+}]$; it is, however, inversely dependent on $[C_2O_4^{2-}]$ (Figure 7). The same first-order rate constant is also obtained when λ_{mon} = 500 nm, where a spectral *decay* is observed (Figure 6).

Thus, the initial and final spectra obtained upon the 266- and 355-nm laser excitation are unquestionably those of $MV^{\bullet+}$ species; however, the differences in these spectra, which are very apparent in Figure 6, argue that the species are not identical. In fact, the final spectrum is virtually identical with the well-known spectrum[54] of $MV^{\bullet+}$ obtained in continuous and flash photolysis, continuous and pulse radiolysis, electrolysis, and thermal reduction and can, indeed, be ascribed to $MV^{\bullet+}$ free in solution. The initial spectrum, on the other hand, shows an enhanced absorption in the 450–500-nm region, reminiscent of that displayed by reduced-viologen dimers and aggregats.[54]

In order to understand the nature and kinetics of the secondary spectral change, which, as $[MV^{2+}]$ is increased, clearly is not due to reaction 6, it is necessary to examine in detail the environment in which $MV^{\bullet+}$ finds itself upon excitation of the $MV^{2+}/C_2O_4^{2-}$ complex. Although the absorption of the complex in the near-UV arises from a species with a 1:1 stoichiometry, consideration must be given to the existence of higher aggregate species that do not contribute to the spectrum. MV^{2+} has been observed, by light-scattering measurements, to form aggregates in neutral aqueous solution at a concentration of about 10 mM;[55] although the presence of Cl^- at 0.1–1 M does not have an appreciable effect on this "critical aggregation concentration" (CAC), 0.1 M phosphate buffer at pH 7 lowers the CAC. The effect of high concentrations of $C_2O_4^{2-}$ on CAC is unknown, but one can surmise that the strong ion-pairing interaction between MV^{2+} and $C_2O_4^{2-}$ lowers CAC significantly (perhaps to 1 mM or below), so that, for the 355-nm laser excitation experiments, MV^{2+} exists mainly as higher ion-paired aggregates. In fact, one can visualize that the aggregated MV^{2+} species exist in a hydrophobic core surrounded by a hydrophilic sheath of $C_2O_4^{2-}$ ions; the structure can be regarded as a "pseudomicelle".

The absorption of light by a $MV^{2+}/C_2O_4^{2-}$ unit within the "pseudomicelle" would generate $MV^{\bullet+}$ and $C_2O_4^{\bullet-}$ therein via the equivalent of reaction 2; unless the latter radical undergoes decarboxylation within the "pseudomicelle" in competition with geminate pair back-electron transfer, no net production of $MV^{\bullet+}$ could occur. The $CO_2^{\bullet-}$ radical thus generated within the "pseudomicelle" could easily reduce a second MV^{2+} in a time much shorter than that required for the reaction to occur diffusionally in homogeneous solution. The result would be the existence of two $MV^{\bullet+}$ units in close proximity, yielding an initial spectrum that would have the characteristics of the reduced "dimer"; it has been suggested recently[56] that $MV^{\bullet+}$ does not dimerize but, rather, aggregates into micelle-like particles. However, now the ion-pairing interaction between $MV^{\bullet+}$ and $C_2O_4^{2-}$ would be less strong than between the original substrates; the $MV^{\bullet+}$ species within the "pseudomicelle" can be visualized to exist in an unstable environment. The slow first-order conversion would be due to the rearrangement of the aggregate structure as $MV^{\bullet+}$ is released into bulk solution in its final relaxed, equilibrated condition. The rate constant for this transformation would be expected to be independent of $[MV^{2+}]$ and the intensity of the laser beam. However, as $[C_2O_4^{2-}]$ is lowered in the bulk solution, the rate of equilibration of the cation radicals would be enhanced; it should be noted that the dynamic breakup of aqueous micelles involving the release of one of the surfactant units occurs on the μs time frame.[57] Scheme I shows the represntation of this model; only two MV^{2+} ions are shown in the core of the "pseudomicelle", and only one $C_2O_4^{2-}$ in the sheath, for simplicity.

Scheme I

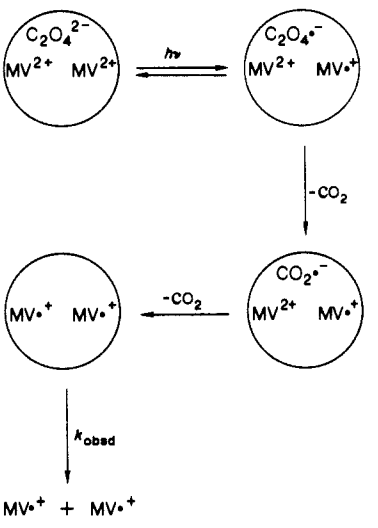

In the 266-nm experiments at lower $[MV^{2+}]$, aggregation would exist to a lesser extent; only a very small contribution of the "pseudomicelle" to the initial spectrum and its slow transformation would be made. $MV^{\bullet+}$ would be produced in two stages in approximately equal amounts from the excitation of the complex and the secondary reaction of $CO_2^{\bullet-}$ in homogeneous solution; by and large, the rate of the latter would be proportional to $[MV^{2+}]$. As $[MV^{2+}]$ is increased, the onset of aggregation would become apparent. For example, the effective concentration of free MV^{2+} would not increase proportionally with the total MV^{2+} concentration, so that the rate of secondary formation of $MV^{\bullet+}$ would not continue to rise linearly but would fall off with increasing $[MV^{2+}]$. Reactions involving the aggregates would not become apparent until they became a large fraction of the total process and rate determining, as is the case in the 355-nm experiments.

Fine-Tuning the Mechanism. Finally, consideration must be given to the effect of aggregation on $\Phi(MV^{\bullet+})$ in continuous photolysis. It would appear that under the conditions of very low $[MV^{2+}]$ that were employed in some of the 254-nm experiments, reactions 2–6 and 12 in homogeneous solution would be operative with η_{cr}, reflecting the competition between reactions 3 or 12 and 4. At higher $[MV^{2+}]$, this same $[MV^{2+},C_2O_4^{2-}]$ absorbing unit would be contained within the "pseudomicelle" aggregate; the processes occurring subsequent to the absorption of a photon are given in Scheme I. The independence of η_{cr} on the concentrations of the substrates at 254 and 340 nm argues that the probability of the breakup of the initially formed geminate pair is largely independent of the environment in which it is found; certainly, there is no analogue to reaction 3 in the "pseudomicelle" model. One is drawn to the inescapable conclusion that the propensity of the caged $C_2O_4^{\bullet-}$ species toward decarboxylation in competition with geminate cage electron transfer is the main factor controlling the value of the cage release yield; a similar conclusion was reached by other workers[58] regarding the dissociative nature of electron capture when tetranitromethane is used as an electron acceptor. This point of view is further supported by the range of values of $\Phi(MV^{\bullet+})$ we have recently observed[59] in the photolysis of ion-pair complexes of MV^{2+} and hydroxycarboxylates, where the charges on all species are the same, but the stabilities of the resulting $RCO_2^{\bullet}$ radicals are different.

(54) Summers, L. A. *The Bipyridinium Herbicides*; Academic Press: London, 1980; Chapter 4.
(55) Ebbesen, T. W.; Ohgushi, M. *Photochem. Photobiol.* **1983**, *38*, 251.
(56) Rieger, A. L.; Rieger, P. H. *J. Phys. Chem.* **1984**, *88*, 5845.
(57) Fendler, J. H. *J. Phys. Chem.* **1985**, *89*, 2730.
(58) Masnovi, J. M.; Huffman, J. C.; Kochi, J. K.; Hilinski, E. F.; Rentzepis, P. M. *Chem. Phys. Lett.* **1984**, *106*, 20.
(59) Prasad, D. R.; Hoffman, M. Z., work in progress.

Acknowledgment. This research was supported in part by grants from the Office of Basic Energy Sciences, Division of Chemical Sciences, U.S. Department of Energy (M.Z.H.) and the National Institutes of Health (M.A.J.R.) and in part by Consiglio Nazionale delle Ricerche of Italy. The collaboration between Q.G.M. and M.Z.H. is part of the U.S.-Italy Cooperative Research Program. CFKR is supported jointly by the Biomedical Research Technology Program of the Division of Research Resources of NIH (RR 008866) and by the University of Texas. The authors thank Dr. S. J. Atherton (CFKR) for technical assistance and many highly stimulating discussions; they also thank Dr. V. Malba and Professor G. Jones (B.U.) for their continued interest in this work.

The $C_{10}H_8$ Potential Energy Surface: The Azulene-to-Naphthalene Rearrangement

Michael J. S. Dewar* and Kenneth M. Merz, Jr.

Contribution from the Department of Chemistry, The University of Texas at Austin, Austin, Texas 78712. *Received February 12, 1986*

Abstract: The azulene-to-naphthalene rearrangement (AN rearrangement) has been studied, using MNDO and MINDO/3. All of the proposed unimolecular pathways have been examined in detail and found wanting. The results presented here agree with the first step of a mechanism proposed by Becker et al. A new mechanism is proposed for the rest of the reaction.

We recently reported[1] a preliminary study of the azulene-to-naphthalene (**1** → **2**) rearrangement (AN reaction) which eliminated from consideration several of the mechanisms that had been previously proposed and we also suggested a new alternative. Here we present the results of a systematic study of the $C_{10}H_8$ potential energy (PE) surface, carried out in the hope of finally solving the problem. We will not discuss its historical developement because an excellent review has recently appeared.[2]

Experimental Procedure

MNDO[3] was used for closed-shell species and the spin-unrestricted version of MNDO[4] (UMNDO) for biradical or open-shell species. All geometries were fully optimized, using the DFP method.[5] In certain cases where MNDO is known to give large errors (e.g., hydrogen transfers), MINDO/3[6] (or UMINDO/3) calculations were also carried out for comparison. All transition states (TS) were located by using the reaction coordinate method,[7] refined by minimizing the norm of the gradient,[8] and characterized by establishing that the Hessian (force constant) matrix had one, and only one, negative eigenvalue.[8] Options for all these procedures are included in the MOPAC package of computer programs.[9]

Results and Discussion

Schemes I and II show the unimolecular mechanisms proposed, respectively, by Scott[10] and Becker,[11] while Scheme III shows the mechanism proposed here on the basis of our calculations. First we will explain why our results eliminate the Scott and Becker mechanisms as possible major contributors to the AN rearrangement. Unfortunately, no mechanism yet proposed, not even the one suggested here, can explain *all* of the results obtained from labeling studies.[12] We have therefore also studied various possible pathways for the scrambling of the labels in azulene and naphthalene in the hope of resolving the remaining discrepancies. This work is presented in the following paper.

Scheme I. The Scott Mechanism

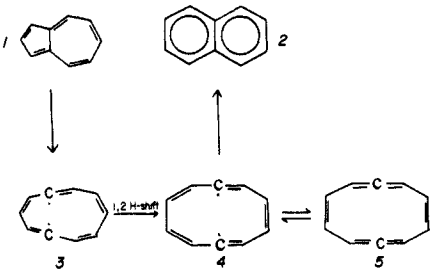

Scheme II. The Becker et al. Mechanism

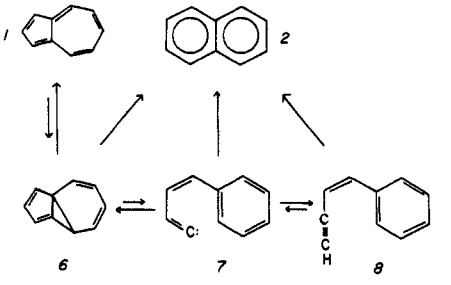

Scheme III. The MNDO Mechanism

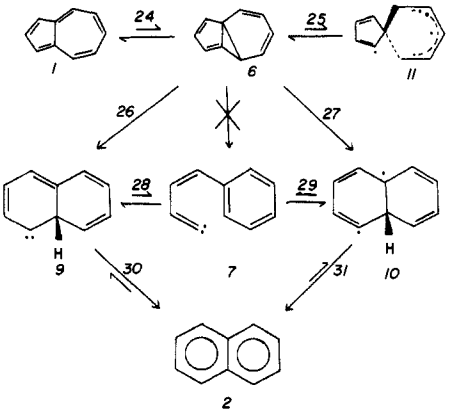

(1) Dewar, M. J. S.; Merz, K. M., Jr. *J. Am. Chem. Soc.* **1985**, *107*, 6111.
(2) Scott, L. T. *Acc. Chem. Res.* **1982**, *15*, 52.
(3) Dewar, M. J. S.; Thiel, W. *J. Am. Chem. Soc.* **1977**, *99*, 4899, 4907.
(4) Pople, J. A.; Nesbet, R. K. *J. Chem. Phys.* **1954**, *22*, 571.
(5) Davidon, W. C. *Comput. J.* **1958**, *1*, 406. Fletcher, R.; Powell, M. J. D. *Comput. J.* **1963**, *6*, 163.
(6) Bingham, R. C.; Dewar, M.J. S.; Lo, D. H. *J. Am. Chem. Soc.* **1975**, *97*, 1285, 1294, 1302, 1307.
(7) Dewar, M. J. S.; Kirschner, S. *J. Am. Chem. Soc.* **1972**, *94*, 2625.
(8) McIver, J. W.; Komornicki, A. *Chem. Phys. Lett.* **1971**, *10*, 303. McIver, J. W.; Komornicki, A. *J. Am. Chem. Soc.* **1972**, *94*, 2625.
(9) QCPE publication 455, Department of Chemistry, Indiana Unversity, Bloomington, IN 47405.
(10) Scott, L. T.; Kirms, M. A. *J. Am. Chem. Soc.* **1981**, *103*, 5875.
(11) Becker, J.; Wentrup, C.; Katz, E.; Zeller, K. P. *J. Am. Chem. Soc.* **1980**, *102*, 5110.
(12) (a) Alder, R. W.; Whittaker, G. J. *J. Chem. Soc., Perkin Trans. 2* **1975**, 714. (b) Alder, R. W.; Whilshire, C. *J. Chem. Soc., Perkin Trans. 2* **1975**, 1464. (c) Alder, R. W.; Whiteside, R. W.; Whittaker, G. J.; Whilshire, C. *J. Am. Chem. Soc.* **1979**, *101*, 629. (d) Zeller, K. P.; Wentrup, C. Z. *Naturforsch. B* **1981**, *36*, 852. (e) Scott, L. T.; Kirms, M. A.; Earl, B. C. *J. Chem. Soc., Chem. Commun.* **1983**, 1373. (f) See ref 2, 10, 11, 16.

0002-7863/86/1508-5142$01.50/0